Swirl Flow Post-CHF Heat Transfer with Refrigerant 113

Seok-Jae Yoo* and D. M. France**

(Received September 11, 1995)

Heat transfer rate was experimentally determined in the post-CHF region of a steady-state two-phase flow of a refrigerant in a vertical tube with swirl induced by twisted-tape inserts. Experiments were performed with the vertical flow of refrigerant-113 in a tube with inside diameter of 7.75 mm, a heated length of 3.66 m and mass flux of 375~535 kg/m^{2}s for swirl flow at a pressure of 0.184 MPa. Four tapes were used with twist-ratio of 2.5 to 9.2 for swirl flow. Liquid heating produced the low wall-superheat in the post-CHF region at steady-state, which is typical of heat exchanger operation. Superheated vapor measured at the test section exit in most tests ensured that entire post-CHF region was included. All refrigerant-113 data were compared with the data of water and refrigerant-12. The existing post-CHF heat transfer correlation of swirl flow was modified to predict the magnitude and trends of the data of the three fluids such as water, R-12 and R-113.

Key Words: Twisted-Tape, Post-CHF, Swirl Flow, Two-Phase Flow, Dispersed Flow

Nomenclature

Bo : Boiling number
CHF : Critical heat flux
c_p : Specific heat
D : Diameter
DAS : Data Acquisition system
F : F Factor
f : Fanning friction factor
G : Mass velocity
g : Acceleration of gravity
h : Heat transfer coefficient
i_{lv} : Latent heat of vaporization
k : Thermal conductivity
L : Length
m : Mass flow rate
Nu : Nusselt number
P : 180° twist pitch
Pr : Prandtl number
q″ : Heat flux at tube inside surface
Re : Reynolds number
T : Temperature
X : Quality
Y : Twist ratio P/D
Z : Axial distance along the test section

Greek Letters

β : Volmetric coefficient of expansion
μ : Viscosity
ρ : Density
ψ : Fraction of tube surface area for wall to drop heat transfer

Subscripts

a : Actual or axial
b : Bulk
b,R-113 : Bulk condition of R-113
CHF : Critical heat flux
H : Hydraulic
h : Heating liquid
i : Inner
l : Liquid
lv : Difference between saturated liquid and vapor
MOD : Modified
o : Outer
s : Shell

* Yong-In Technical College, 449-890 Yong-In gun Yong-In up Mapyung Ri 77-1 Kyung Ki Do, South Korea
** The University of Illinois at Chicago, Department of Mechanical Engineering (M/C 251), P. O. Box 4348, Chicago, Illinois 60680, USA

sat : Saturated
v : Vapor
v, a : Vapor condition evaluated at axial condition
v, s : Vapor condition based on swirl condition
w : Wall
wi : Inner wall
wo : Outer wall

1. Introduction

Many systems in which fluids are boiled to saturated or superheated vapor can benefit from the use of heat transfer augmentation devices or surfaces. Heat transfer augmentation is especially attractive for the case where the critical heat flux (CHF) is exceeded in internal forced convective flows. Augmentation devices that produce a swirl component in single-phase flows have been found by Rabas (1989) to be quite efficient (compared to other augmentation mechanisms) in increasing heat transfer rates. These devices also can be successful in increasing heat transfer rates in the post-CHF region of two-phase flows. Here vapor occupies the predominant volume of the flow structure as the continuous phase, and a discrete liquid phase is present in the form of entrained drops. Important applications of such devices are in refrigeration and air-conditioning evaporators where there can be substantial size reduction benefits. However, the majority of studies on heat transfer augmentation have been conducted for single-phase fluids (Bergles et al., 1979), and nearly all of the post-CHF studies have concentrated on axial flow rather than swirl flow as reviewed by Koai et al. (1985), Wang and Weiseman (1983) and George and France (1991).

The objective of the present experimental investigation is to study heat transfer in the post-CHF regime under swirl flow conditions for heat exchanger application. This two-phase flow regime is especially amenable to heat transfer augmentation because the heat transfer coefficient is low compared to the annular flow regime both of which typically exist in refrigeration evaporators. Of specific interest to this investigation are twisted-tape inserts inside of vertical tubes which generate the swirl flow condition.

2. Swirl Flow Post-CHF

Early experiments into post-CHF heat transfer with twisted-tape inserts were performed by Bergles et al. (1971) at cryogenic temperatures and low mass fluxes in the range of 30-140kg/m^{2}s. Assuming thermodynamic equilibrium in the swirling flow, a superposition of heat transfer rates between the vapor and the heated wall and between the liquid drops and the wall was used in developing a correlation of the data. The superposition takes.

$$q''=[\Psi h_{l-w}+(1-\Psi)h_{v-w}](T_w-T_{sat}) \quad (1)$$

where Ψ is the fraction of tube surface area associated with direct wall-to-liquid-drop heat transfer. The heat transfer coefficient h_{l-w} was adapted from the work of Baumeister et al. (1966). And the heat transfer coefficient h_{v-w} was adapted from the work of Thorsen and Landis (1968) which was based on high wall-superheat data similar to the tests of Bergles et al. (1971).

The correlation was modified by Papadapoulos et al. (1993) for the low wall superheat conditions using the single-phase vapor, swirl flow, heat transfer correlation of Lopina and Bergles (1968) which was developed from data with wall superheats in the range of 6-78℃. The correlation is

$$(1-\Psi)N_{v-w}=f\left[0.0195Re_{v,s}^{0.8}Pr_v^{0.4}+0.083\left\{\left(\frac{Re_{v,a}}{Y}\right)^2\left(\frac{D_H}{D}\right)\beta_v(T_w-T_{sat})Pr_v\right\}^{\frac{1}{3}}\right] \quad (2)$$

Where the swirl velocity for twisted-tape-induced swirl is

$$V_s=\frac{V_a}{2Y}(4Y^2+\pi^2)^{0.5} \quad (3)$$

All properties are evaluated at the fluid bulk temperature unless the film temperature is specified. The tape-twisted ratio Y is a pitch to diameter ratio based on the length of 180 degree of twist and the tube diameter.

For the droplet contribution, Bergles et al. (1971)

modified the correlation of Baumeister et al. (1966) to account for the different acceleration field, which was expressed as follows

$$\Psi h_{l-w}=1.1\left[\frac{k_v^3 i_{lv}^* a\rho_l\rho_v}{(T_w-T_{sat})\mu_v\left(\frac{\pi}{6}\right)^{\frac{1}{3}}}\right]^{\frac{1}{4}}\left[\frac{(1-X)\frac{6}{\pi}}{X\left(\frac{\rho_l}{\rho_v}-1\right)+1}\right]^{\frac{2}{3}}\frac{\pi}{4}F\left(\frac{a}{g}\right) \tag{4}$$

where the rotating slug flow acceleration and velocity are

$$a=\frac{(V_a\pi)^2}{2DY^2} \tag{5}$$

$$V_a=\frac{G}{\rho_l}\left[1+X\left(\frac{\rho_l}{\rho_v}-1\right)\right] \tag{6}$$

and

$$i_{lv}^*=i_{lv}\left[1.0+\frac{7}{20}\frac{c_{p,v}(T_w-T_{sat})}{i_{lv}}\right]^{-3} \tag{7}$$

The factor F(a/g) accounts for the effect of the radial velocity of the liquid drops towards the heated wall. Papadapoulos et al. (1991) did extensive work on dispersed flow film boiling with swirl. He assumed thermodynamic equilibrium in the swirling flow and used the superposition of heat transfer between the vapor and the heated wall and between the liquid drops and wall. The study of Papadapoulos et al. (1991) utilized experiments of Carlson et al. (1986) in high pressure water (15.9 MPa) with liquid heating and twisted tape swirl generators. The correlation of heat transfer by Lopina and Bergles (1969) which was developed from data with wall superheats in the range of 6-78℃ shown in Eq. (2) was used in place of the higher superheat-based equation of Thorsen and Landis (1968). For the heat transfer between drops and wall, the correlation of Bergles et al. (1971) in Eq. (4) was used. The wall superheats were below 41℃ and the mass fluxes were relatively high ranging from 910 to 1878 kg/m²s. As a result of the high mass fluxes of these water experiments, the drop acceleration was much larger than in the work of Bergles et al. (1971), and the contribution to heat transfer due to drop-wall interaction was modified by Papadopoulos to include both an acceleration and a quality effect. The F factor in Eq. (4) was modified as follows

$$F=1.749\left(\frac{a}{g}\right)^{0.6557}\left\{\frac{1-X}{\frac{(1+X_{CHF})}{2}}\right\} \tag{8}$$

Later Papadapoulos et al. (1991) used R-12 to simulate water at high pressure and high mass fluxes typical of steam generator conditions. The mass flux of R-12 covered the range of 100-1000 kg/m²s. Improvement was obtained by modification to Eq. (8) retaining the Lopina and Bergles (1969) single-phase liquid correlation. Eq. (2) for low wall-superheat as done successfully by Papadapoulos et al. (1991).

At high mass fluxes, the F factor was modified from Eq. (8)

$$F=0.42\left(\frac{a}{g}\right)^{1.15}\left\{\frac{1-X}{\frac{(1+X_{CHF})}{2}}\right\}^{0.5} \tag{9}$$

Papadapoulos et al. (1993) found that the data were better correlated if the mass flux effect was diminished and the effect of heat flux was included. Therefore, a final modification was made to the correlation developed for swirl flow post-CHF heat transfer. Both parameters were applied through the Boiling number Bo changing Eq. (1) to

$$q''=C[\Psi h_{l-w}+(1-\Psi)h_{v-w}]\cdot(1000Bo)^{0.4}(T_w-T_{sat}) \tag{10}$$

where C is a constant. Since the wall temperature appears explicitly in the individual phase heat transfer coefficients of Eq. (10), the heat flux was introduced indirectly resulting in a heat transfer coefficient h for the two-phase swirl flow based on T_w-T_{sat} of

$$h=0.4917[\Psi h_{l-w}+(1-\Psi)h_{v-w}]^{1.67}\cdot\left[\frac{1000(T_w-T_{sat})}{Gi_{lv}}\right]^{0.67} \tag{11}$$

3. Experimental Facility and Operation

3.1 Design features

The Flow Boiling Facility (FBF) was designed

and operated in the Boiling Heat Transfer Laboratory at University of Illinois at Chicago. It was constructed to obtain more understanding of two-phase flow heat transfer phenomena. It was also designed in a way that the teat section can be easily changed without modifying the whole facility.

In contrast to commonly used electrically heated test sections, the liquid heating of the FBF was designed to operate under heat exchanger conditions. Closed pumped fluid circuits are used for the boiling fluid (R-113) and the heating fluid (water). Heat was supplied to the water by a series of electric resistance heaters in the flow circult. There are advantages and disadvantages of liquid heating in post-CHF heat transfer experimentation. Advantageous features are: it is closer to actual applications; it generates less severe temperatures; and it gets the full extent of the post-CHF region. Compared with electrical heating, however, fluid heating requires long test section and more elaborate data acquisition techniques.

3.2 Test section

A schematic diagram of the FBF showing the flow processes is given in Fig. 1. and the test section is given in Fig. 2. The length of test section is 3.66 m and it is a counter flow concentric single tube heat exchanger with upward flow of working fluid (R-113) in the inner tube and downward flow of heating (water) in the annulus. The test section shown in Fig. 2 was made of copper with inner tube inside diameter of 7.75 mm, tube wall thickness of 0.885 mm and annulus outer diameter of 16.56 mm represents the lower limit of the actual range of inner tube inside diameter of nuclear steam generators. At the bottom of the test section, there is U-shape tubing which is removable so that twisted tapes can be inserted through the inner R-113 tube. Between the U-tube section and the test section, there is a

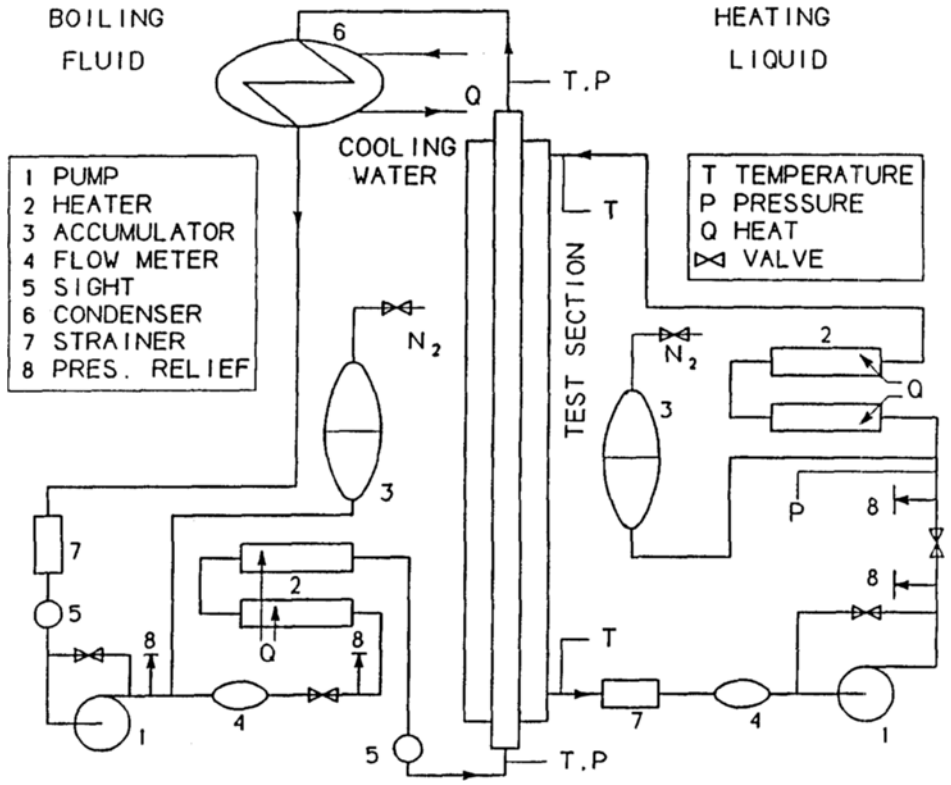

Fig. 1 Schematic drawing of Flow Boiling Facility (FBF)

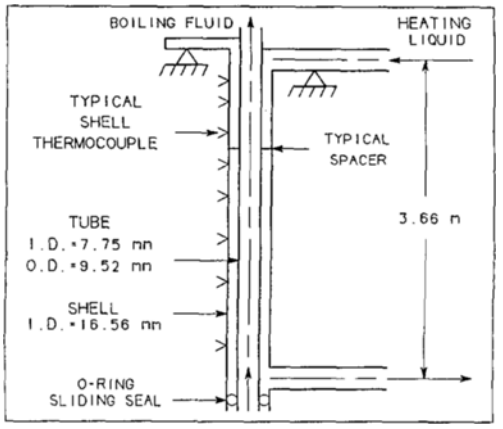

Fig. 2 Test section

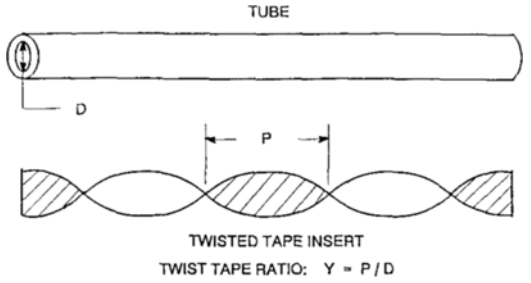

Fig. 3 Schematic drawing of a twisted tape

0.9 m long tube assembly which has two o-ring seals where the inner tube and outer tube can slide with respect to one another to accommodate differential thermal expansion. The shell and tube test section remained concentric by using 5 sets of spacers located 60.9 cm apart axially. The whole test section was insulated with fiber glass 6 cm thick.

3.3 Twisted tape

Generally, a twisted tape insert is characterized by the features shown in Fig. 3. The severity of the helical twist is usually referred to by a dimensionless twist ratio, $Y=P/D$. The twisted tape used in this study was made of brass which is compatible with the test section material employed to avoid electrochemical phenomena when exposed to a high temperature medium. The width of tape was 0.75 cm and thickness 0.05 cm which provided a loose enough fit to be pulled with ease through the tube yet tight enough prevent by-pass flow past the tape.

4. Data Acquisition and Reduction

Steady-state conditions, determined from analog recordings of test section stream temperatures and flow rates, were established at prescribed test parameters. Data were then accumulated on computer disk for later processing. A data scan consisted of measurements of the 57 shell temperatures plus 10 measurements of flow rates, pressures, and test section stream temperatures. The 10 measurements were averaged for each sensor in the post-test data reduction to eliminate any electronic noise that might be present. The shell thermocouples were not averaged because CHF movement would seriously affect the accuracy in the post-CHF region. The shell thermocouple readings were taken in less than 2 s, and the time for a complete data scan and data transfer to the computer was 25 s. Other parameters along the length of test section were calculated from these data after testing was completed.

The local heat flux in a liquid-heated system is calculated from shell temperature measurements and the heating fluid flow rate and properties. Several options are available, and results of a detailed investigation of many of them showed that a relatively straightforward approach will provide good accuracy in the post-CHF region where axial heat flux gradients are not large. Gradient method was utilized in the present study after the shell temperature measurements were smoothed with cubic splines. The heat flux to the boiling fluid at the tube inside surface q″ was calculated from the gradient of the shell temperatures as

$$q''=\frac{m_h C_{p,h}}{\pi D_i}\frac{dT_s}{dZ} \tag{12}$$

Based on fully developed flow, hydraulically and thermally, it was assumed that the shell temperature is approximately equal to the bulk temperature. Therefore, with this assumption, the wall temperature of the outside of the boiling fluid tube T_{wo} was calculated from

$$q''=\frac{h_o D_o}{D_i}(T_s-T_{wo}) \tag{13}$$

The annulus heat transfer coefficient at the boiling tube h_o was determined experimentally using the Wilson plot technique for a series of experiments performed with R-113 in the liquid state. The Monrad correlation was found to represent the annulus data well, and it was used in the analysis of the subsequent boiling tests. The Monrad and Pelton correlation is

$$\frac{h_o(D_s-D_o)}{k_h}=0.02Re_h^{0.8}Pr_h^{1/3}\left(\frac{D_s}{D_o}\right)^{0.53} \quad (14)$$

A sensitivity check was performed on the use of Monrad and Pelton equation. The annulus heat transfer coefficient was reduced by 15% from the correlation value, and the data were reanalyzed. The Monrad and Pelton correlation (1942) was also found to predict water heat transfer well in an annulus in a similar temperature range. Data controls included test section heat balance calculations for the liquid R-113 tests and for the boiling tests where a substantial exit vapor-superheat was measured by a stream thermocouple indicating that thermal equilibrium had been achieved. These heat balances were within 5% and mostly less than 2%. The calculations were made using temperatures and flows measured by the DAS and constituted an end-to-end calibration verification. After the heat flux was determined in a boiling test, the boiling fluid enthalpy and equilibrium quality were calculated along the test section length from a heat balance. The boiling fluid equilibrium temperature was found from the pressure and enthalpy. The tube wall temperature at the inside surface T_{wi} was found from a one dimensional (radial) conduction model for the tube, and the equilibrium heat transfer coefficient was then determined based on this temperature and the boiling fluid equilibrium temperature. This procedure was followed for 10 tests covering the mass flux range of 375 to 535 kg/m²s. A typical plot is given in Fig. 4 in the direction of the boiling fluid flow. The open symbols shown in Fig. 4 represent the measured shell temperatures, and the solid line represents the cubic spline fit to them. The peak in the heat flux marks CHF. The boiling fluid temperature (bulk temperature in Fig. 4) is seen to be approximately constant at a saturation temperature of 77℃ (in this and all other tests) until reaching superheat (under the condition of thermodynamic equilibrium) at approximately 2.1 m beyond the inlet. The post-CHF data between the CHF point and the start of equilibrium vapor superheat were analyzed from all of the tests performed.

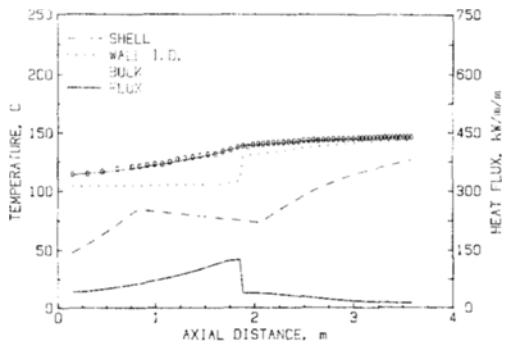

Fig. 4 Swirl flow data at G=468 kg/m²s, Y=2.5

5. Results and Discussion

5.1 Test parameters

During all tests, it was important that the annulus water flow be turbulent to ensure a high heat transfer coefficient so that the thermal resistance of the water was not large with respect to the post-CHF region. Also, it was important to establish a sizable temperature drop more than 30℃ on the water shell side of test section for good sensitivity of result. Cumo's liquid heated experiments possessed small heating liquid temperature differences that rendered the local results noninterpretable (1974).

5.2 Swirl flow experiments

A typical plot of local parameters along the length of the test section (in the direction of R-113 flow) from a boiling test is given in Fig. 4 the open symbols shown in Fig. 4 represent the measured shell temperature, and the solid line is the cubic spline fit to them. The peak in the heat flux makes CHF. The swirl flow tests of this study displayed similar trends to those of the open tube. The shell temperatures and the heat flux in each case showed a sharp change at CHF just as the open tube. As shown in Fig. 4 the wall tempera-

ture sharply increased about 25℃ at the CHF point, and the heat flux dropped about 70 kW/m² after the CHF point because of the absence of liquid in contact with wall. Fig. 4 also shows a slight increase in heat flux in the post-CHF region compared with the superheated region. The post-CHF region is defined between the sharp increase of wall temperature and the position in the tube where the quality equals to one and the bulk temperature increases above saturation. The high swirl in the flow accelerated the drops towards the wall and extended the length of annular flow to X=1 in this case. This condition is common at low mass flux and tighter twist ratios. The presence of the tapes increases an already high X_{CHF}. This is a positive factor for the application to once through steam generators where operation in the post-CHF is very important to the design.

The bulk temperature of the heating fluid (water) increased approximately linearly as function of distance from the start of the post-CHF region as shown by the shell temperature in Fig. 4. This results in a near constant heat flux in the region as seen in Fig. 4.

5.3 Swirl flow correlation

Tests were performed with twist ratios varying from 2.5 to 9.2 and mass fluxes from 375kg/m²s to 535kg/m²s. The radial acceleration in the swirl flow is proportional to $(G/Y)^2$ and is an important parameter influencing drop-wall heat transfer. The radial acceleration of R-113 as function of mass flux from experimental data as seen in Fig. 5 was much larger for R-113 compared to previous experimental data for water and R-12. The accelerations of three fluids were from experimental data. As shown in Fig. 5, the acceleration of R-113 increases exponentially as mass flux increases. The F factor which is function of

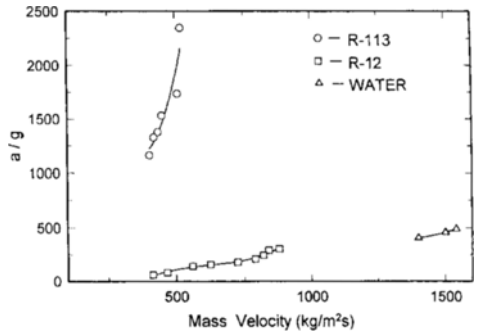

Fig. 5 Comparison of a/g with three fluids

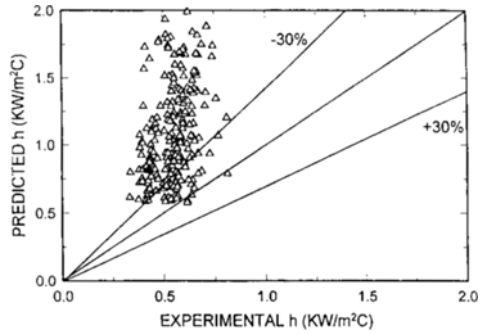

Fig. 6 Prediction of papadopoulos correlation with R-113 experimental data

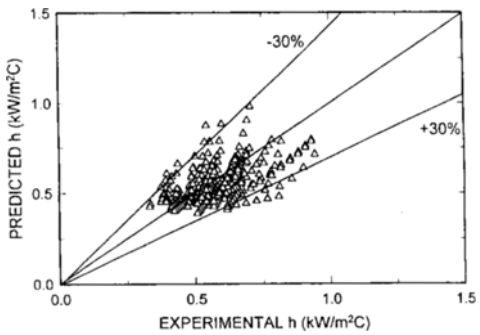

Fig. 7 Prediction of modified correlation with R-113 experimental data

Table 1 Variable range of swirl flow data

Fluid	G(kg/m²s)	$(T_w - T_{wMAX}℃)$	P/Pc	Y	ρ_l/ρ_v	Heating Method
Water	900–1900	40	0.7	2–15	5.48	Liquid
R-12	100–1000	50	0.25	2–10	20	Liquid
R-113	375–535	50	0.054	2–10	99	Liquid

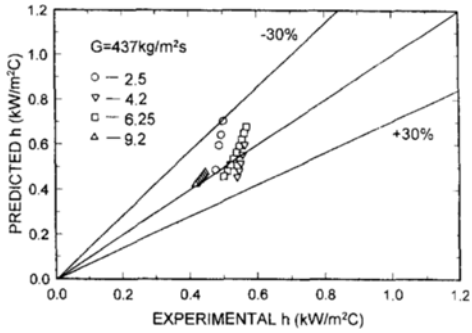

Fig. 8 Comparison of four twisted tape results at constant mass flux (G=437kg/m²s)

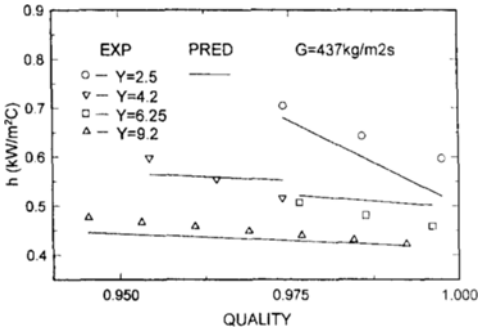

Fig. 9 Comparison of four twisted tape results at constant mass flux (G=437kg/m²s)

acceleration and quality in the correlation of Papadapoulos et al. (1993) was significantly large for R-113 data and the correlation of Papadapoulos et al. (1993) highly overpredicted the experimental data points of R-113 as shown in Fig. 6. As the acceleration of R-113 increases exponentially with the increase of mass flux, it can be expected that the F factor in Eq. (9) and heat transfer coefficient h in Eq. (11) can be expressed as exponential functions. To cover the large values of acceleration, the F factor which is a function of acceleration in Eq. (9) was modified as exponential function and h in Eq. (11) were modified also to best fit the R-113 data as follows

$$F = C_1 \exp\left\{ 4.425 - C_2 \left(\frac{a}{g}\right)^{1.1} \right\} (a/g)^{1.1} \cdot \left[\frac{2(1-X)}{(1+X_{CHF})} \right]^{0.5} \tag{15}$$

$$h_{MOD} = C_h [\, \Psi h_{l-w} + (1-\Psi)\, h_{v-w} \,]^{1.67} \cdot \left[\frac{1000(T_w - T_{sat})}{G i_{lv}} \right]^{0.67} \tag{16}$$

where the coefficients for R-113 are $C_1=0.0017$, $C_2=0.00033$, $C_h=0.37$. The heat transfer prediction with modified Eqs. (15)~(16) agreed well with the trends and magnitudes of the data as seen in Fig. 7 for R-113 swirl flow post-CHF.

A comparison of R-113 data with different twist ratios at constant mass flux is shown in Fig. 8. It is seen that no systematic error exists. Local comparisons of R-113 data with four tapes at constant mass flux are shown in Fig. 9 as a composite.

5.4 Correlations with three fluids

All post-CHF data of R-113 are well predicted with modified F factor as an exponential function and with modified coefficient of h_{MOD}. From the correlation of R-113 with the modified F factor and modified coefficient of h_{MOD}, it can be inferred that the other fluids also can be expressed as exponential functions. The modified constants for water and two refrigerants are given in Table 2. All coefficients of the modified F factor and coefficient h_{MOD} in Table 2 are expressed as functions of the ratio of liquid to vapor density. The coefficients of the modified F factor, C_1 and C_2 in Eq. (15) are linear as function of (ρ_l/ρ_v) as seen in Figs. 10 and 11 for three fluids. The coefficients C_1 and C_2 as function of (ρ_l/ρ_v) are

Table 2 Constants for modified equation with three fluids

Fluid	C_1	C_2	C_h	ρ_l/ρ_v	Pressure
R-113	0.0017	0.00033	0.37	99	184kPa
R-12	0.008	6×10^{-5}	0.4917	20	1014 kPa
Water	0.009	10^{-5}	0.52	5.48	6897 kPa

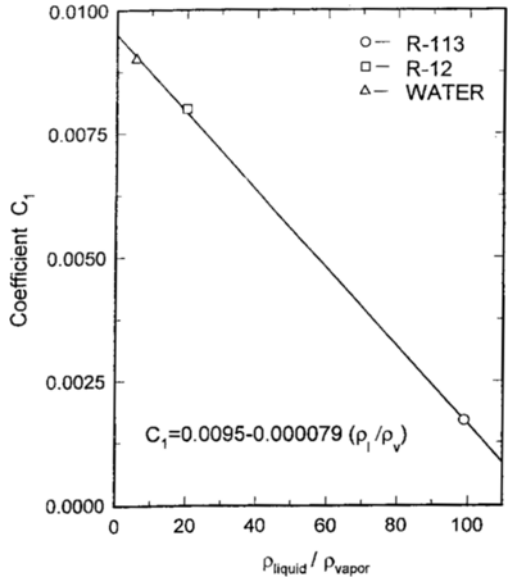

Fig. 10 Comparison of coefficient C_1 in Eq. (17) with three fluids

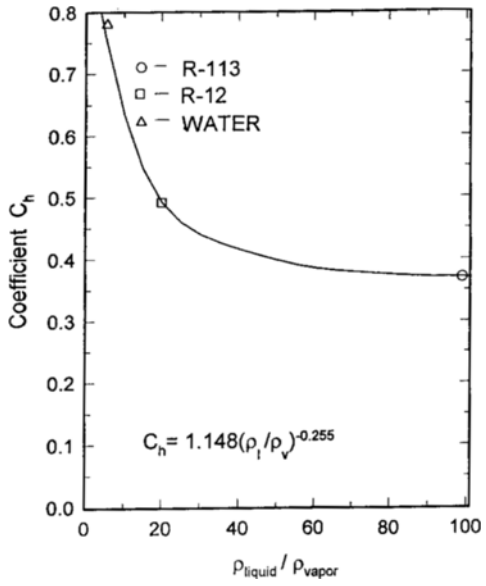

Fig. 12 Comparison of coefficient C_h in Eq. (19) with three fluids

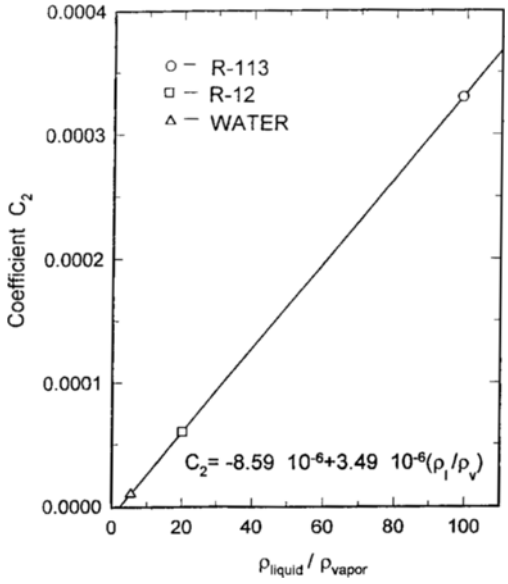

Fig. 11 Comparison of coefficient C_2 in Eq. (18) with three fluids

$$C_1 = 0.0095 - 7.9 \times 10^{-5}\left(\frac{\rho_l}{\rho_v}\right) \tag{17}$$

$$C_2 = \left[-8.59 + 3.49\left(\frac{\rho_l}{\rho_v}\right) \right] \times 10^{-6} \tag{18}$$

The coefficient C_h of h_{MOD} in Eq. (16) decreases as function of (ρ_l/ρ_v) as shown in Fig. 12. The coefficient C_h can be expresed as follows

$$C_h = 1.148\left(\frac{\rho_l}{\rho_v}\right)^{-0.255} \tag{19}$$

The modified equations of Papadapoulos et al. (1993) are Eqs. (15) and (16) which predict the data of three fluids well with the parameters expressed as function of (ρ_l/ρ_v) as follows

$$F = \left[0.0095 - 7.9 \times 10^{-5}\left(\frac{\rho_l}{\rho_v}\right) \right] \cdot \exp\left[4.425 - \left\{ -8.59 + 3.49\left(\frac{\rho_l}{\rho_v}\right) \right\} \times 10^{-6}\left(\frac{a}{g}\right)^{1.1} \right] \left(\frac{a}{g}\right)^{1.1} \left[\frac{2(1-X)}{(1+X_{CHF})} \right]^{0.5} \tag{20}$$

$$h_{MOD} = 1.148\left(\frac{\rho_l}{\rho_v}\right)^{-0.255} \left[\Psi h_{l-w} + (1-\Psi) h_{v-w} \right]^{1.67} \left[\frac{1000(T_w - T_{sat})}{Gi_{lv}} \right]^{0.67} \tag{21}$$

where Ψh_{l-w} is from Eq. (4) and $(1-\Psi)h_{v-w}$ is from Eq. (2).

This form of the Papadapoulos correlation now predicts post-CHF swirl flow heat transfer over a large fluid parameter range. Commonly used fluids of water and refrigerants form the data base. Fluids with properties encompassed by these three fluids are expected to be predicted well also.

6. Conclusions

The effect of swirl on post-CHF heat transfer was studied in a flow boiling facility (FBF) experimentally at low wall superheats. A fluid, R-113, was used as the working fluid, and the data were compared with those of water and R-12. Ninety five experiments for swirl flow were run in the FBF. Swirl flow post-CHF heat transfer experiments performed with a new fluid R-113 produced very high a/g compared to other fluids (water and R-12), and existing correlation were inadequate in predicting the data. Drop wall heat transfer of R-113 was high compared to other two fluids as expected due to high a/g and previous correlation did not account for this effect. Heat transfer correlation was modified to predict data of three fluids (water, R-12, R-113) covering wide mass flux range and four twisted-tape ratios of 2. 5 to 9.2 The drop wall heat transfer term was developed as an exponential function which includes the high a/g of R-113 and predicts the data of the other two fluids well also.

References

Bergles, A. E., Fuller, W. D. and Hynek, S. J., 1971, Dispersed Flow Film Boiling of Nitrogen with Swirl Flow, *Int. J. Heat Mass Transfer*, Vol. 14, pp. 1343~1354.

Bergles, A. E., Webb, R. L., Junkham, G. H. and Jensen, M. K., 1979, Bibliography on Augmentation of Convective Heat and Mass Transfer, Htl-19, ISU-ERI-Ames-79206, Iowa State University, Ames, Iowa.

Baumeister, K. J., Hamill, T. D. and Schoessow, G. J., 1966, A Generalized Correlation of Vaporization times of Drops in Film Boiling on a flat plate, *Proceedings of the 3rd International Heat Transfer Conference*, Vol. Ⅳ, AICHE, pp. 66~73.

Carlson, R. D., France, D. M. and Gabler. M. J., 1986, Heat Transfer Augmentation in Liquid Metal Reactor Steam Generators, Proceedings of the 1986 Joint ASME/and Nuclear Power Conference, ANS, pp. 211~217.

Cumo, M., Farello, G. E. and Palazzi, G., 1974, The Influence of Twisted-Tapes in Subcritical Once-Through Vapor Generators in Counter Flow, *J. Heat Transfer*, Vol. 96, pp. 365~370.

George, C. M. and France, D. M., 1991, Post-CHF Two-Phase Flow with Low Wall Superheat, *Nucl. Engrg. Des.*, Vol. 125, pp. 97~109.

George, C. M. and France, D. M., 1991, Post-CHF Two-Phase Flow with Low Wall Superheat, *Nucl. Engrg. Des.*, Vol. 125, pp. 97~109.

Koai, K. K., Vazone. A. F. and Rohsenow. W. M., 1985, Comparison of Post-Dryout Heat Transfer Prediction methods, *U.S.A.-Japan Joint Symposium on Heat Transfer, San Diego.*

Lopina. R. F. and Bergles, A. E., 1969, Heat Transfer and Pressure Drop in Tape Generated Swirl Flow of Single-Phase Water, *J. Heat Transfer*, Transactions, *ASME*, pp. 434~445, Aug.

Monrad, C. C. and Pelton, J. F., 1942, Transactions of the AICHE 34.

Papadopoulos, P., France, D. M. and Minkowycz, W. J., 1991, Heat Trnsfer to Dispersed Swirl Flow of High Pressure Water with Low Wall-Superheat, *Experimental Heat Transfer*, Vol. 4, pp. 153~169.

Papadopoulos, P., Chang, C., France, D. M. and Minkowycz, W. J., 1991, Mass Flux Effects in Post-CHF Swirl Heat Transfer, Int. Comm, Heat Mass Transfer, Vol. 18, pp. 297~307.

Papadopoulos, P., France, D. M., Minkowycz, W. J., Harty, J., Wu, M.-S. and Hamoudeh, N., Two-phase Dispersed Flow Heat Transfer Augmented by Twisted Tapes, Submitted for Publication to *J. of Enhanced Heat Transfer*.

Rabas, T. J., 1989, Selection of the Energy-Efficient Enhancement Geometry for Single-Phase Turbulent Flow Inside Tubes : Heat Transfer Equipment Fundamentals, Design, Applications and Operation Problems, *ASME*, New York, HTD-Vol. 108, pp. 193~204.

Thorsen, R. and Landis, F., 1968, Friction and Heat Transfer Characteristics in Turbulent Swirl Flow Subjected to Large Transverse Temperature Gradients, *J. Heat Transfer*, Vol. 90, pp. 87~98.

Wang, S. W. and Weisman, J., 1983, Post-

Critical Heat Flux Heat Transfer: A Survey of Current Correlations and Their Appliability, *Progress in Nuclear Energy*, Vol. 12, pp. 149 ~168.